Supplementary Table S1. Characteristics of the AML patients with HLA class II downregulation at post-transplantation relapse considered in the study

Patient Code	UPN01	UPN02	UPN03	UPN04	UPN05
Sex	F	M	M	M	F
Age at Transplant (y)	25	54	52	52	65
Disease Diagnosis	AML De Novo	AML De Novo	AML De Novo	AML De Novo	t-AML
Cytogenetics	normal	normal	normal	normal	n.e.
Molecular Alterations	DNMT3A, NPM1 mutA, FLT3-ITD	NPM1 mutA	DNMT3A, NPM1mutA, IDH2	NPM1mutA, FLT3-ITD	-
Status at Transplant	CR1	AD	AD	AD	CR1
Type of Donor	Matched Unrelated	Family Haploidentical	Family Haploidentical	Family Haploidentical	Matched Unrelated
Donor-Recipient HLA Matching	10/10	5/10	5/10	5/10	10/10
Conditioning Regimen†	Flu-Bu4	Thio-Treo-Flu	Treo-Flu	Thio-Treo-Flu	Treo-Flu
***In vivo* T cell Depletion**	ATG	PT-Cy	PT-Cy	PT-Cy	ATG
Graft Source	PBSC	PBSC	PBSC	PBSC	BM
$CD34^+$ cells infused/Kg*10^6	5.01	6.00	7.97	8.52	1.28
$CD3^+$ cells infused/Kg*10^6	286.6	300.0	274.88	353.0	19.1
Post-transplantation GvHD Prophylaxis	CsA+MMF	Sir+MMF	Sir+MMF	Sir+MMF	Sir+MMF
aGvHD	no	no	no	no	no
cGvHD	no	no	no	no	no
Time to Relapse (d)	33	90	57	83	346

Abbreviations: F=female; M=male; AML=Acute Myeloid Leukemia; t-AML=Therapy related-Acute Myeloid Leukemia; CR1=First Complete Remission; AD=Active Disease; PBSC=Peripheral Blood Stem Cells; BM=Bone Marrow; ATG=Anti-Thymocyte Globulin; PT-Cy=Post-Transplant Cyclophosphamide; CsA=Cyclosporine A; MMF=Mycophenolate Mofetil; Sir=Sirolimus; aGvHD=acute Graft-versus-Host Disease; cGvHD=chronic Graft-versus-Host Disease.

† Conditioning Regimens: Flu-Bu4: Fludarabine (30 mg/m^2/day on day -6 to -2) and i.v. Busulfan (3.2 mg/kg/day on day -6 to -3); Thio-Treo-Flu: Thiotepa (5 mg/kg/day on day -3 and -2), Treosulfan (14 g/m^2/day on day -6 to -4) and Fludarabine (30 mg/m^2/day on day -6 to -2); Treo-Flu: Treosulfan (14 g/m^2/day on day -6 to -4) and Fludarabine (30 mg/m^2/day on day -6 to -2).

Supplementary Table S2. Characteristics of the AML patients with relapse after sole chemotherapy considered in the study

Patient Code	UPN06CT	UPN07CT	UPN08CT	UPN09CT	UPN10CT
Sex	F	F	M	M	M
Age at Diagnosis (y)	65	74	25	77	65
Disease Diagnosis	AML De Novo	AML De Novo	AML De Novo	AML De Novo	sAML
Cytogenetics	normal	dup(13)	t(8;21)	normal	normal
Molecular Alterations	biallelic CEBPA	-	cKIT	NPM1mutA, FLT3-ITD	-
Chemotherapy Cycles†	3+7	3+7 A8	3+7 MAMAC5	3+7 MAMAC3, A8 Auto-HCT	3+7 A8 (x2)
Time from Last Treatment to Relapse (d)	116	485	30	128	516

Abbreviations: F=female; M=male; AML=Acute Myeloid Leukemia; sAML= secondary Acute Myeloid Leukemia; Auto-HCT=autologous hematopoietic cell transplantation.
† Conditioning Regimens: 3+7: Daunorubicin (60 mg/m^2/day on day 1 to 3) and AraC (100 mg/m^2/day on day 1 to 7); A8: AraC (1 g/m^2/12h on day 1 to 4); MAMAC5: Amsacrine (100 mg/m^2/day on day 1 to 5) and AraC (1 g/m^2/12h on day 1 to 5); MAMAC3: Amsacrine (100 mg/m^2/day on day 1 to 3) and AraC (1 g/m^2/12h on day 1 to 3).

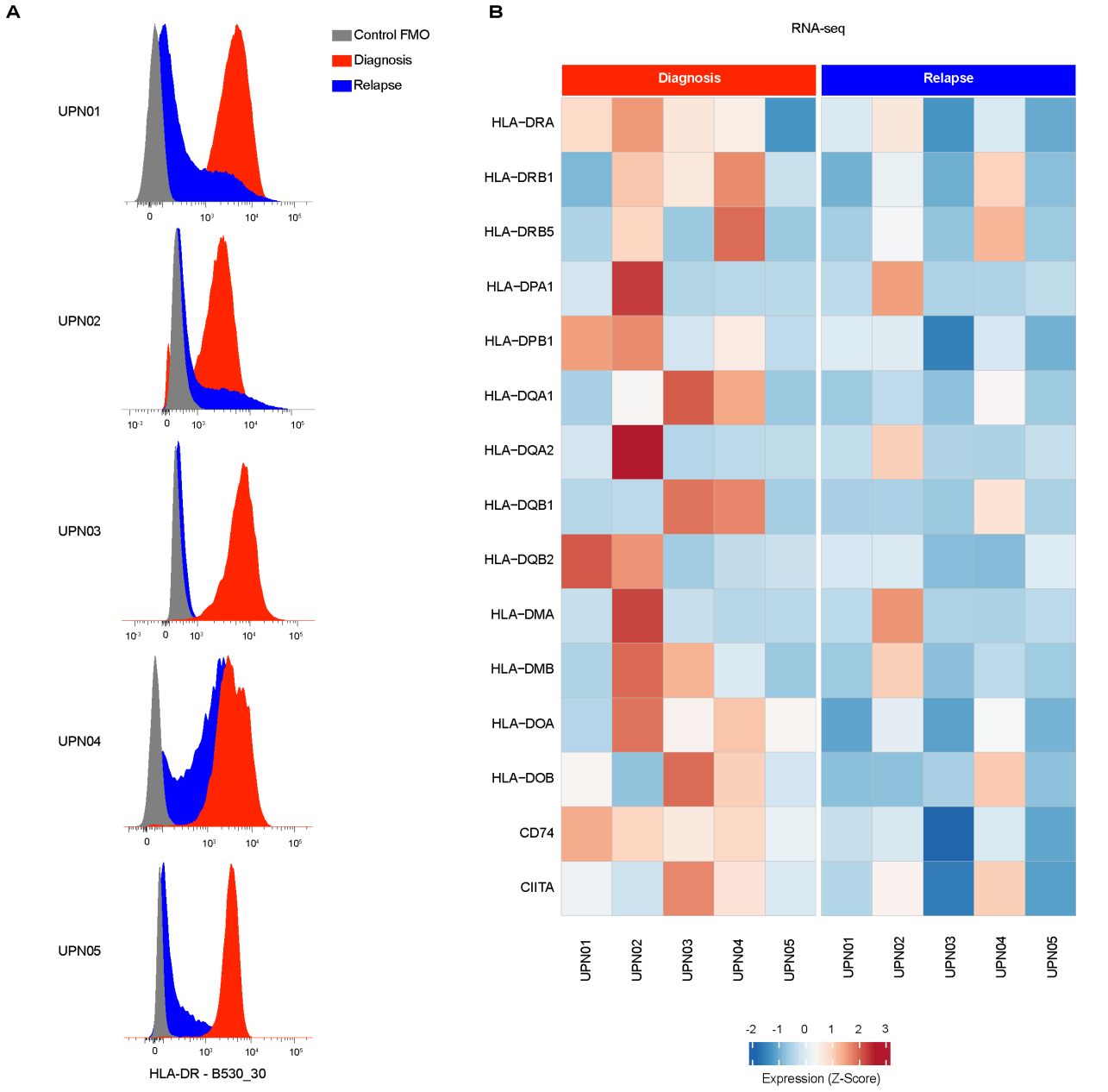

Supplementary Figure S1. Downregulation of HLA class II in the five post-transplantation relapses under study **A.** HLA-DR surface expression measured by immunophenotypic analysis on primary diagnosis (red) and post-transplantation relapse (blue) samples from the five patients under study. Gray histograms indicate fluorescence minus one (FMO) controls from diagnosis samples, not stained for HLA-DR. **B.** Heatmap showing expression of HLA class II genes and of their regulators CD74 and CIITA, measured by RNA-seq in paired primary diagnosis/relapse samples from the five patients under study. The bar above the graph indicates diagnosis (red) and relapse (blue) samples. **C.** Average fold change in the expression of HLA class II-related genes shown in panel B between relapse and diagnosis samples from the five patients under study.

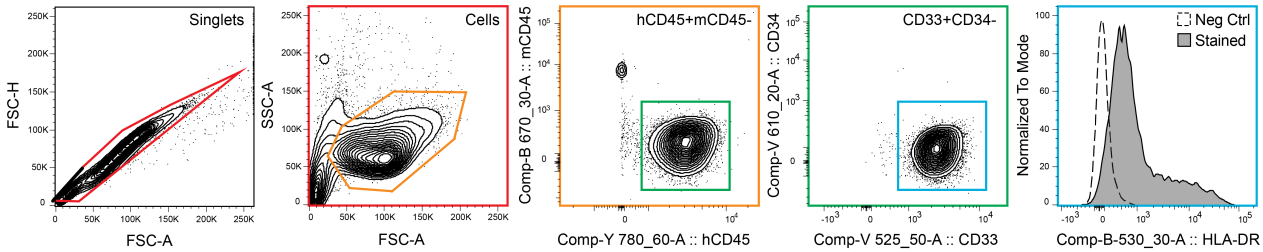

Supplementary Figure S2. Gating strategies for the immunophenotypic analysis of immune markers of interest on leukemic blasts from PDXs or primary samples, representatively exemplified for HLA-DR. Shown are representative flow cytometry plots with the sequential logical gates. After exclusion of doublets (red gate), live cells were gated according to physical parameters (orange gate). Based on the expression of human CD45 (hCD45), human hematopoietic cells were discriminated from murine hematopoietic cells (mCD45, green gate). The human CD45 leukemia population was further defined by its expression of CD33 and CD34 (cyan gate). In this population, we determined the expression of HLA-DR, HLA-ABC, PD-L1 and B7-H3 (gray filled histogram). To exclude the autofluorescence of the markers of interest, a negative control was generated using only lineage markers (hCD45, mCD45, CD33, CD34, CD3, CD14, dashed white histogram).

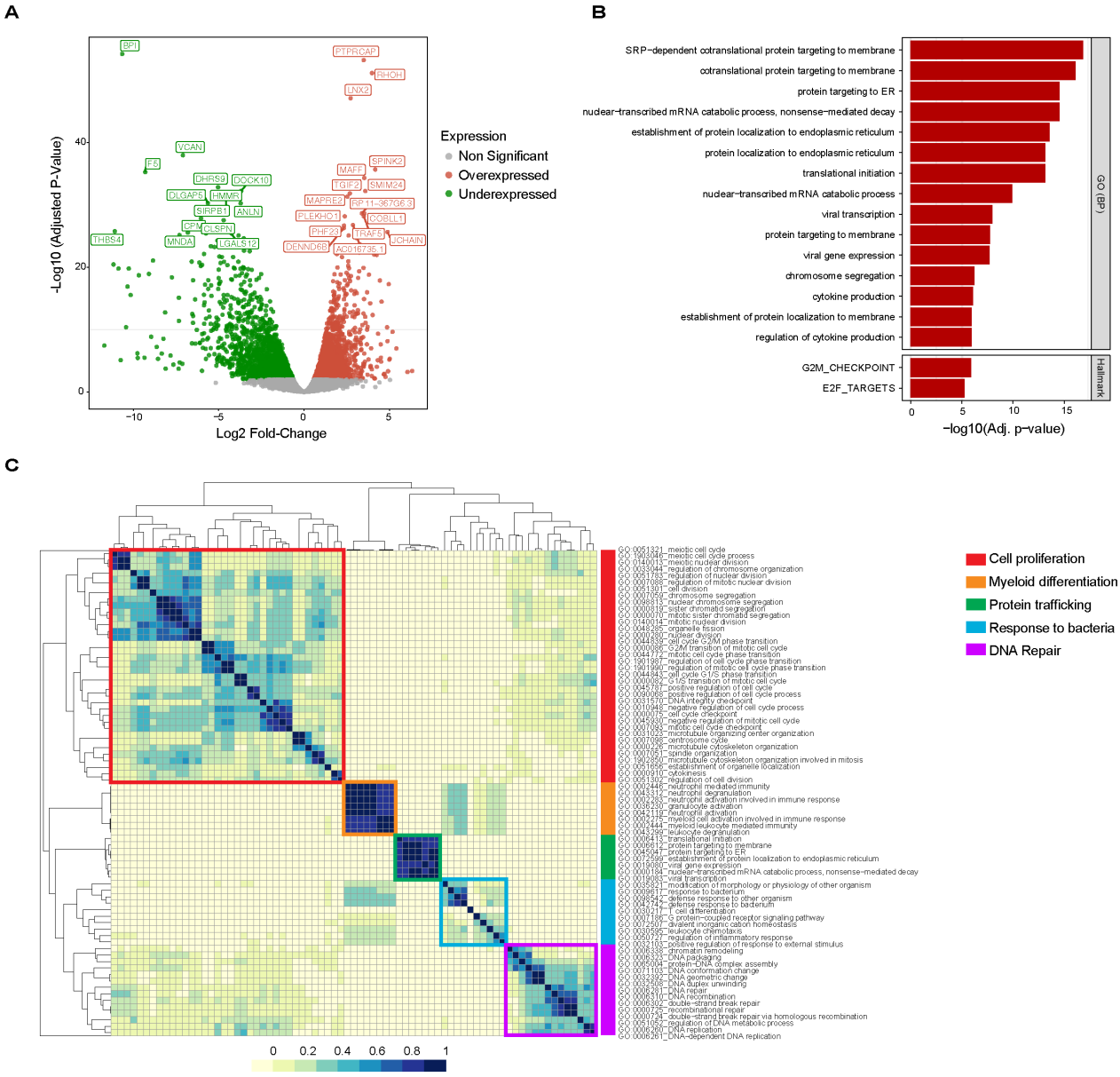

Supplementary Figure S3. Genes and biological processes differential between primary and PDX-derived AML samples. **A.** Volcano plot showing genes significantly down- (green) and up- (red) regulated in AML cells purified from PDXs as compared to their original primary counterpart. Top 30 genes ranked by false discovery rate (FDR) are indicated. **B.** Histogram displaying the Gene Ontology biological processes (GO-BP) and Hallmark Signatures significantly enriched for genes differentially expressed between AML PDXs and their original primary counterpart. Bar lengths indicate significance of the enrichment. **C.** Heatmap representing the semantic similarity between GO terms identified as significantly deregulated (P<0.05) from the comparison between AML-PDX and primary samples. Cell color represents the extent of similarity (blue: high, yellow: low). GO terms are clustered according to their semantic distance, and grouped in deregulated 'macroprocesses' (colored squares in the heatmap).

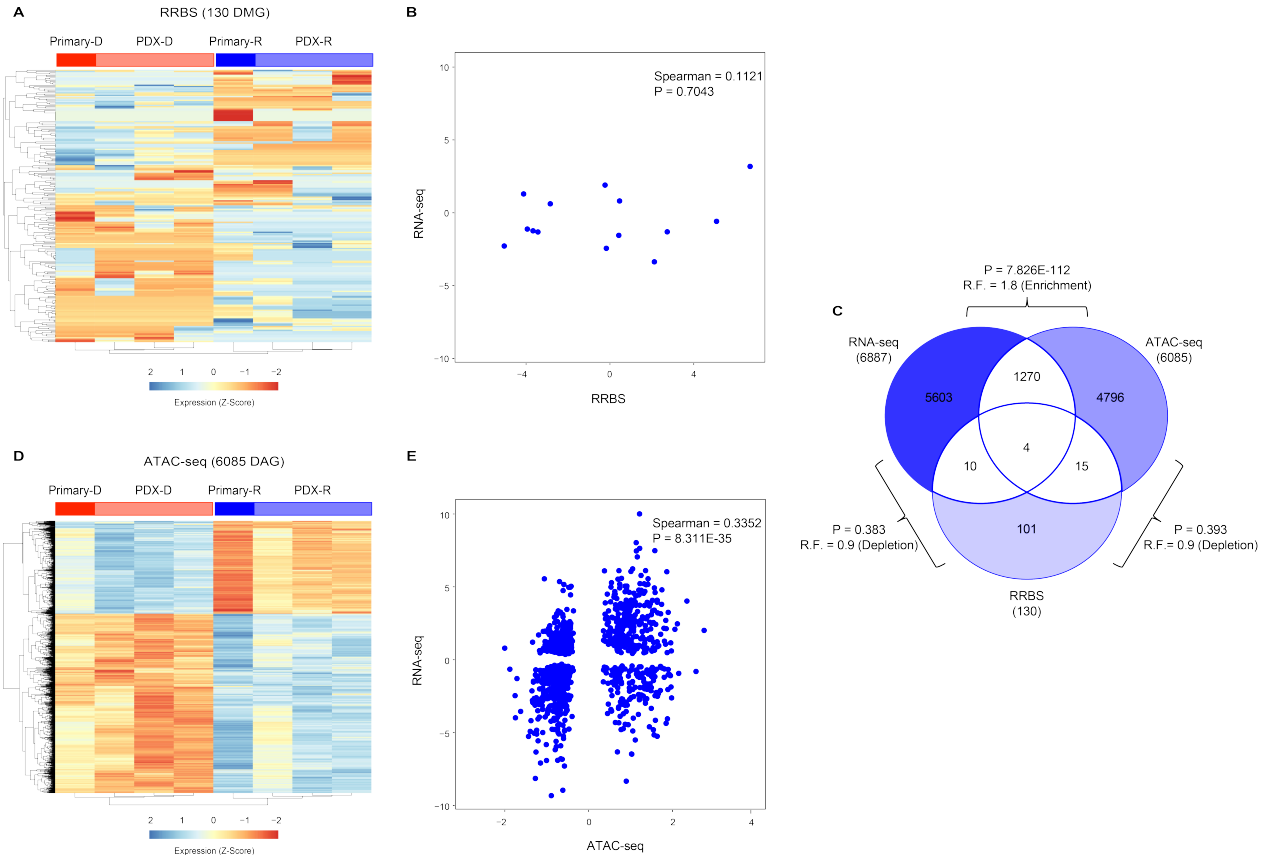

Supplementary Figure S4. Correlation between changes in gene expression, DNA methylation and chromatin accessibility. **A.** Heatmap representing expression levels, measured by RNA-seq, of the 130 differentially methylated genes (DMG) obtained by the comparison of RRBS data from diagnosis and relapse samples from UPN01. The bar above the graph indicates primary (dark colors) and PDX (light colors), diagnosis (red) and relapse (blue) samples. **B.** Correlation between expression levels (measured by RNA-seq, y axis) and extent of gene methylation (measured by RRBS, x axis) in genes that were differentially expressed and methylated between UPN01 diagnosis and relapse. Two-sided P value (95% confidence interval) of Spearman rho coefficient is reported. **C.** Venn diagrams showing the overlap between genes that were differentially expressed (as measured by RNA-seq, n=6887), methylated (as measured by RRBS, n=130) and accessible (as measured by ATAC-seq, n=6085) between UPN01 diagnosis and relapse samples. P values of hypergeometric tests are reported. The representation factor (RF) is the number of overlapping genes divided by the expected number of overlapping genes drawn from two independent groups. **D.** Heatmap representing expression levels, measured by RNA-seq, of the 6085 differentially accessible genes (DAG) obtained by the comparison of ATAC-seq data from diagnosis and relapse samples from UPN01. The bar above the graph indicates primary (dark colors) and PDX (light colors), diagnosis (red) and relapse (blue) samples. **E.** Correlation between expression levels (measured by RNA-seq, y axis) and chromatin accessibility (measured by ATAC-seq, x axis) in genes that were differentially expressed and accessible between UPN01 diagnosis and relapse. Two-sided P value (95% confidence interval) of Spearman rho coefficient is reported.

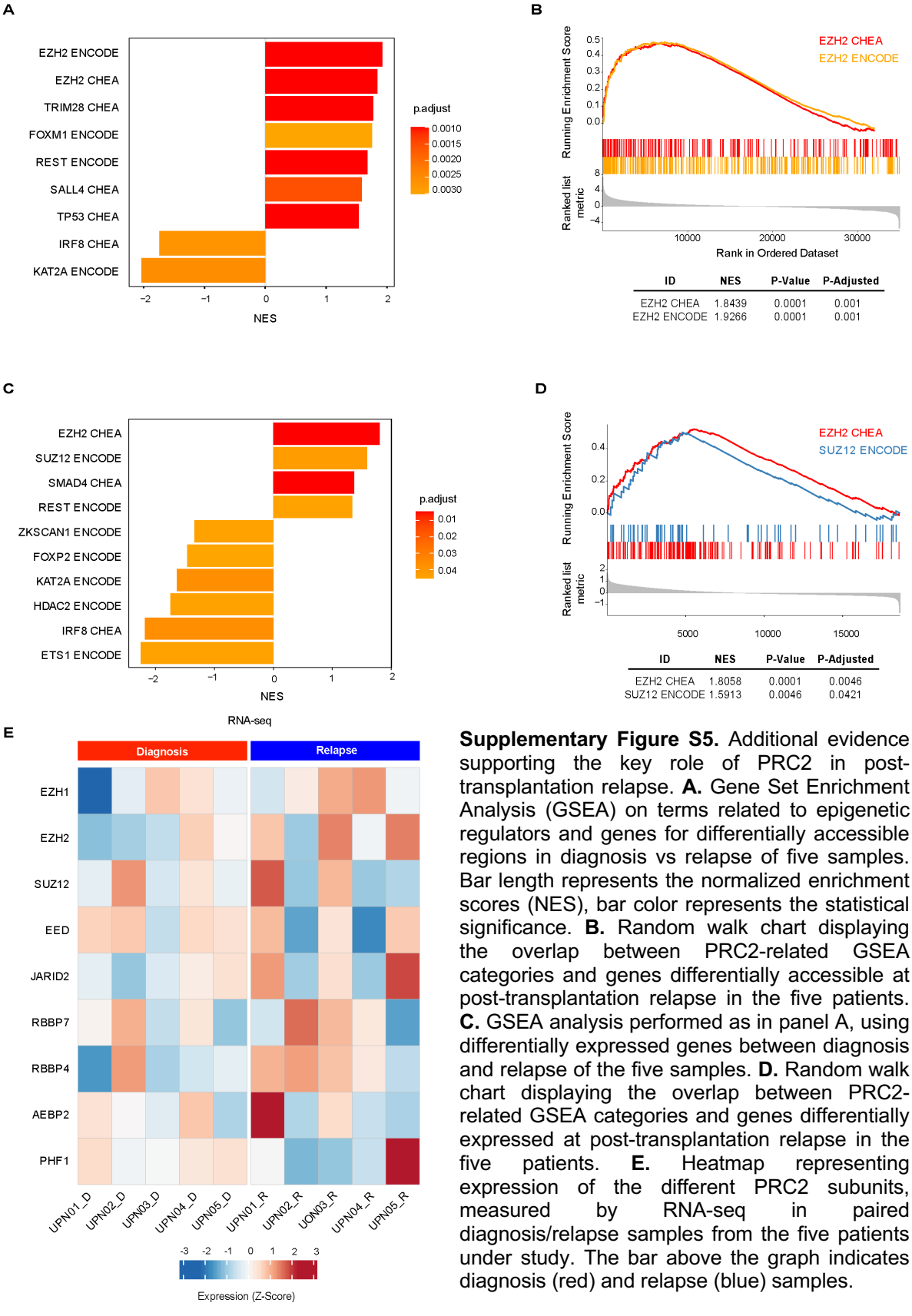

Supplementary Figure S5. Additional evidence supporting the key role of PRC2 in post-transplantation relapse. **A.** Gene Set Enrichment Analysis (GSEA) on terms related to epigenetic regulators and genes for differentially accessible regions in diagnosis vs relapse of five samples. Bar length represents the normalized enrichment scores (NES), bar color represents the statistical significance. **B.** Random walk chart displaying the overlap between PRC2-related GSEA categories and genes differentially accessible at post-transplantation relapse in the five patients. **C.** GSEA analysis performed as in panel A, using differentially expressed genes between diagnosis and relapse of the five samples. **D.** Random walk chart displaying the overlap between PRC2-related GSEA categories and genes differentially expressed at post-transplantation relapse in the five patients. **E.** Heatmap representing expression of the different PRC2 subunits, measured by RNA-seq in paired diagnosis/relapse samples from the five patients under study. The bar above the graph indicates diagnosis (red) and relapse (blue) samples.

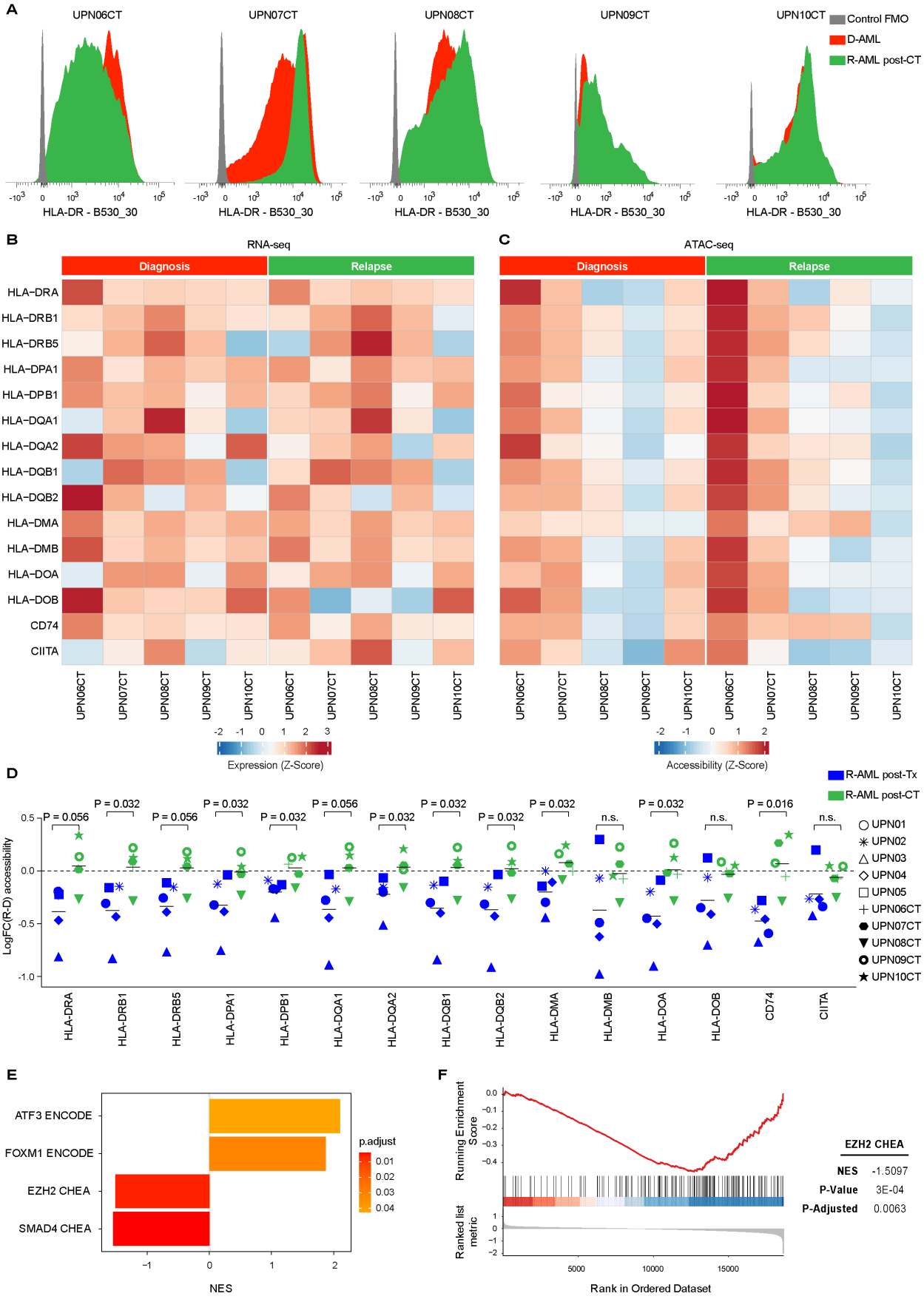
A
UPN06CT
UPN07CT
UPN08CT
UPN09CT
UPN10CT
Control FMO
D-AML
R-AML post-CT
HLA-DR - B530_30
B
RNA-seq
Diagnosis
Relapse
HLA-DRA
HLA-DRB1
HLA-DRB5
HLA-DPA1
HLA-DPB1
HLA-DQA1
HLA-DQA2
HLA-DQB1
HLA-DQB2
HLA-DMA
HLA-DMB
HLA-DOA
HLA-DOB
CD74
CIITA
Expression (Z-Score)
C
ATAC-seq
Accessibility (Z-Score)
D
R-AML post-Tx
R-AML post-CT
LogFC(R-D) accessibility
P = 0.056
P = 0.032
P = 0.016
n.s.
UPN01
UPN02
UPN03
UPN04
UPN05
UPN06CT
UPN07CT
UPN08CT
UPN09CT
UPN10CT
E
ATF3 ENCODE
FOXM1 ENCODE
EZH2 CHEA
SMAD4 CHEA
p.adjust
NES
F
Running Enrichment Score
Ranked list metric
Rank in Ordered Dataset
EZH2 CHEA
NES -1.5097
P-Value 3E-04
P-Adjusted 0.0063

Supplementary Figure S6. HLA class II expression and chromatin accessibility in relapses after sole chemotherapy **A.** HLA-DR surface expression measured by immunophenotypic analysis on primary diagnosis (red) and post-chemotherapy relapse (green) samples from the five control cases who were not exposed to allo-HCT. Gray histograms indicate fluorescence minus one (FMO) controls from diagnosis samples, not stained for HLA-DR. **B.** Heatmap representing expression of HLA class II genes and of their regulators CD74 and CIITA, measured by RNA-seq in paired diagnosis/relapse samples from the five control cases treated with chemotherapy only. The bar above the graph indicates diagnosis (red) and relapse (green) samples. **C.** Heatmap representing accessibility of HLA class II genes and of their regulators CD74 and CIITA measured by ATAC-seq in paired diagnosis/relapse samples from the five control cases who received chemotherapy only. The bar above the graph indicates diagnosis (red) and relapse (green) samples. **D.** Dot plot displaying the difference in HLA class II gene chromatin accessibility between relapse and diagnosis AML samples from patients who received allo-HCT (blue) or chemotherapy only (green). P values were calculated by a two-sided Mann-Whitney test at a 95% confidence interval (CI). **E.** Histogram outlining association between epigenetic regulator Gene Set Enrichment Analysis (GSEA) categories and genes found by ATAC-seq to be differentially accessible between the primary diagnosis and relapse samples from the five control cases who received chemotherapy only. The length of each bar is proportional to the GSEA normalized enrichment score (NES), and intensity of the color to the significance. **F.** Random walk chart displaying the overlap between PRC2-related GSEA categories and genes found by ATAC-seq to be differentially accessible between the primary diagnosis and relapse samples from the five control cases who relapsed after chemotherapy only.

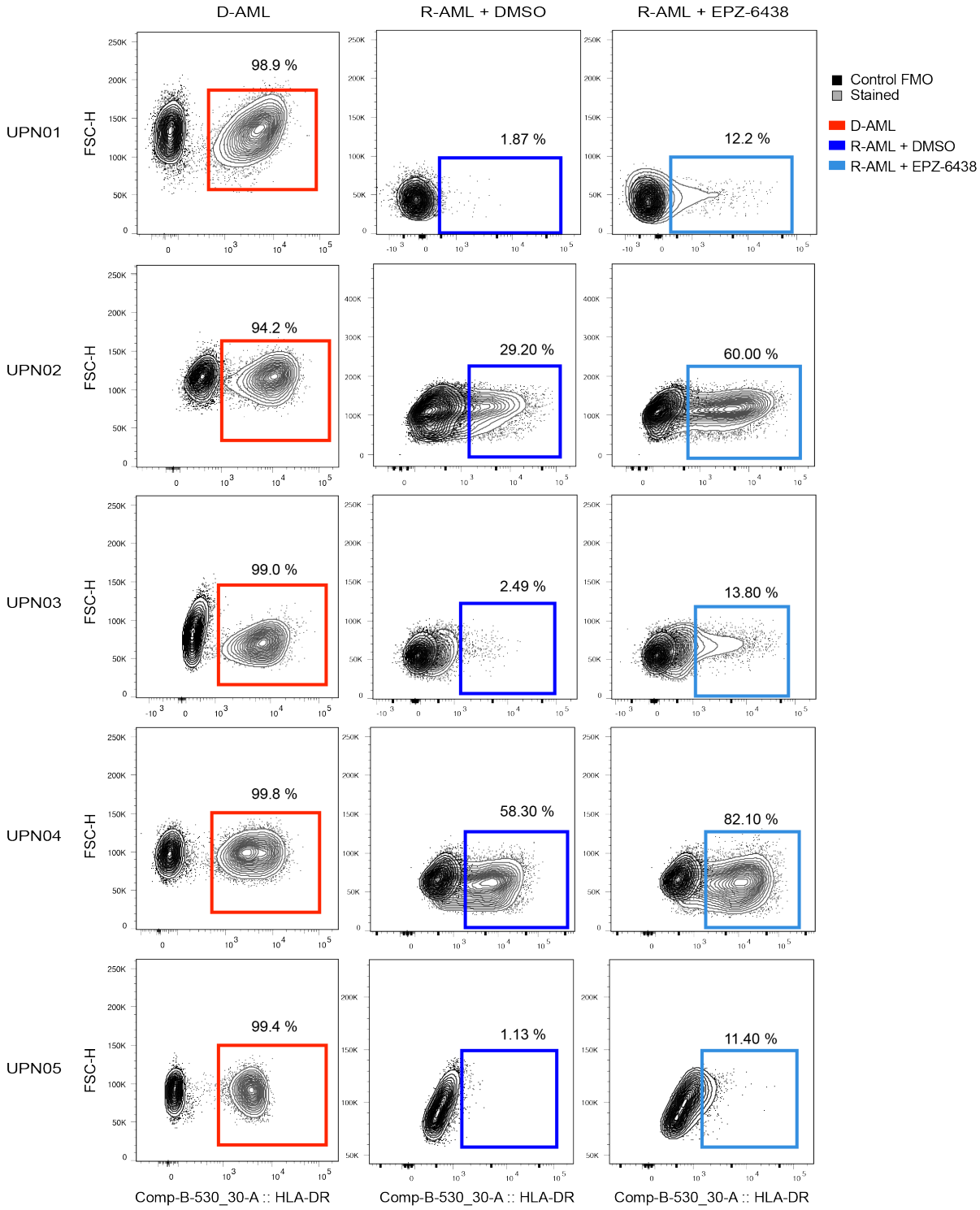

Supplementary Figure S7. HLA class II surface expression in AML cells cultured in presence of the EZH2 inhibitor EPZ-6438. FACS contour plots displaying HLA-DR expression upon logical gating on leukemia cells, in samples collected at diagnosis (leftmost column, HLA-DR$^+$ cells boxed in red) and at relapse after allo-HCT (center and rightmost column, HLA-DR$^+$ cells boxed in blue) from the five patients under study. The rightmost plots show expression of HLA-DR in leukemia cells collected at post-transplantation relapse and cultured for 7 days in the presence of EPZ-6438 at the 10μM concentration. Contour plots from samples stained with the fluoroconjugated anti-HLA-DR mAb are displayed in gray, and the respective FMO controls, not stained for HLA-DR, in black.

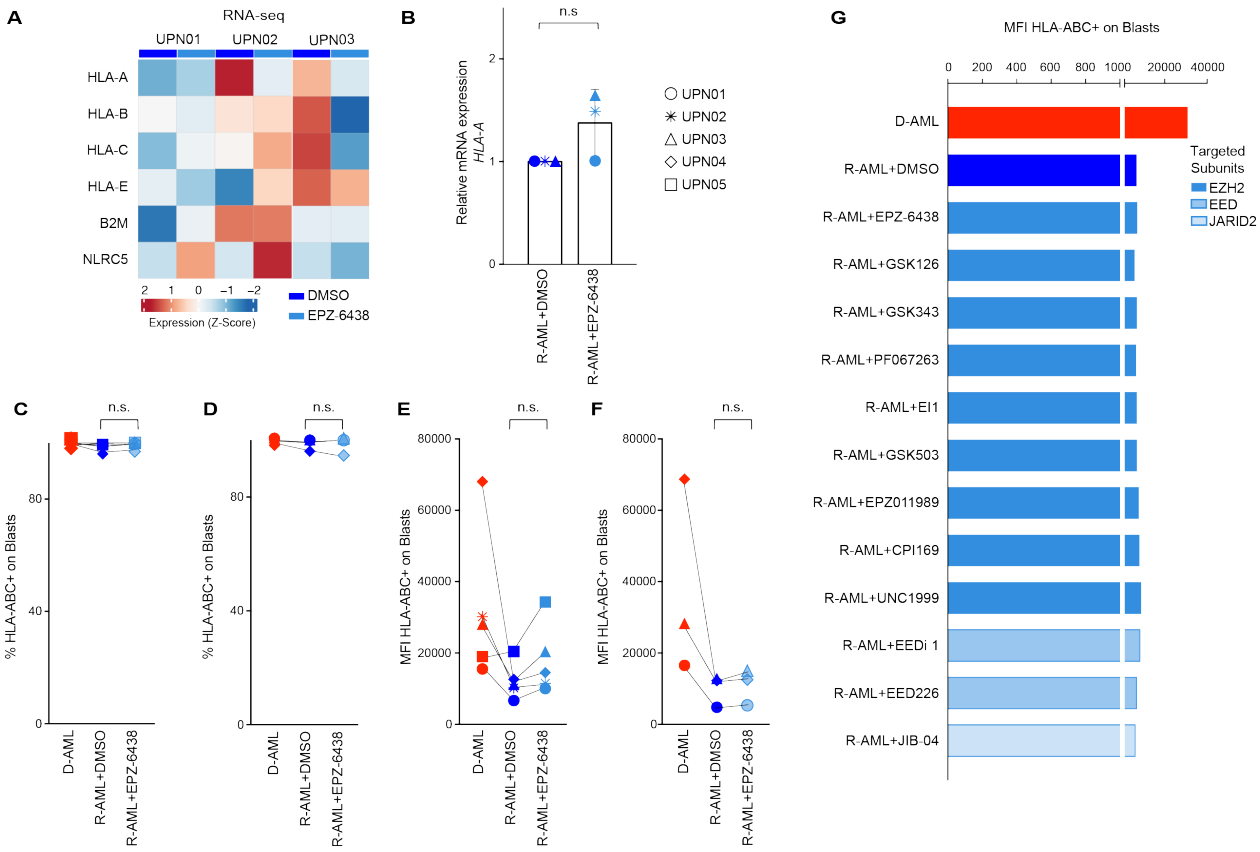

Supplementary Figure S8. Analysis of HLA class I expression upon exposure of relapsed leukemia to PRC2 inhibitors. **A.** Heatmap representing levels of expression of transcripts encoding for HLA class I genes, β2-microglobulin and their regulator NLRC5 measured by RNA-seq in primary relapse samples from UPN01, UPN02 and UPN03 cultured for 7 days with MS-5 stromal cells alone (dark blue markers in the bar above the heatmap) or with the addition of EPZ-6438 (light blue markers in the bar above the heatmap). **B.** mRNA expression level of the *HLA-A* transcript measured by locus-specific quantitative PCR in PDXs generated from relapses of the indicated patients treated with DMSO diluent alone (dark blue symbols) or with 10μM of EPZ-6438 (light blue symbols) for 7-days. Underlying white bars indicate the average fold change in expression relative to DMSO control, and whiskers indicate standard deviation. P value was calculated by a two-sided paired t test at a 95% confidence interval (CI). **C,D.** Immunophenotypic analysis showing the percentage of HLA-ABC$^+$ leukemic blasts from PDXs generated from diagnosis (red) and relapse (blue) samples of different patients cultured for 7 days in the presence of DMSO diluent alone, with EPZ-6438 (panel **C**) or with EED226 (panel **D**). P values were calculated by a two-sided paired t test at a 95% confidence interval (CI). **E,F.** Immunophenotypic analysis showing the mean fluorescence intensity of HLA-ABC$^+$ leukemic blasts from PDXs generated from diagnosis (red) or relapse (blue) samples of different patients cultured for 7 days in the presence of DMSO diluent alone, with EPZ-6438 (panel **E**) or with EED226 (panel **F**). P values were calculated by a two-sided paired t test at a 95% confidence interval (CI). **G.** Immunophenotypic analysis showing the percentage of HLA-ABC$^+$ leukemic blasts from UPN01 diagnosis (red) or relapse (blue) PDXs cultured for 7 days in the presence of DMSO diluent alone or with different PRC2 inhibitors, all used at 10μM concentration. Shades of the blue color of the bars correspond to the PRC2 subunits targeted by the compound.

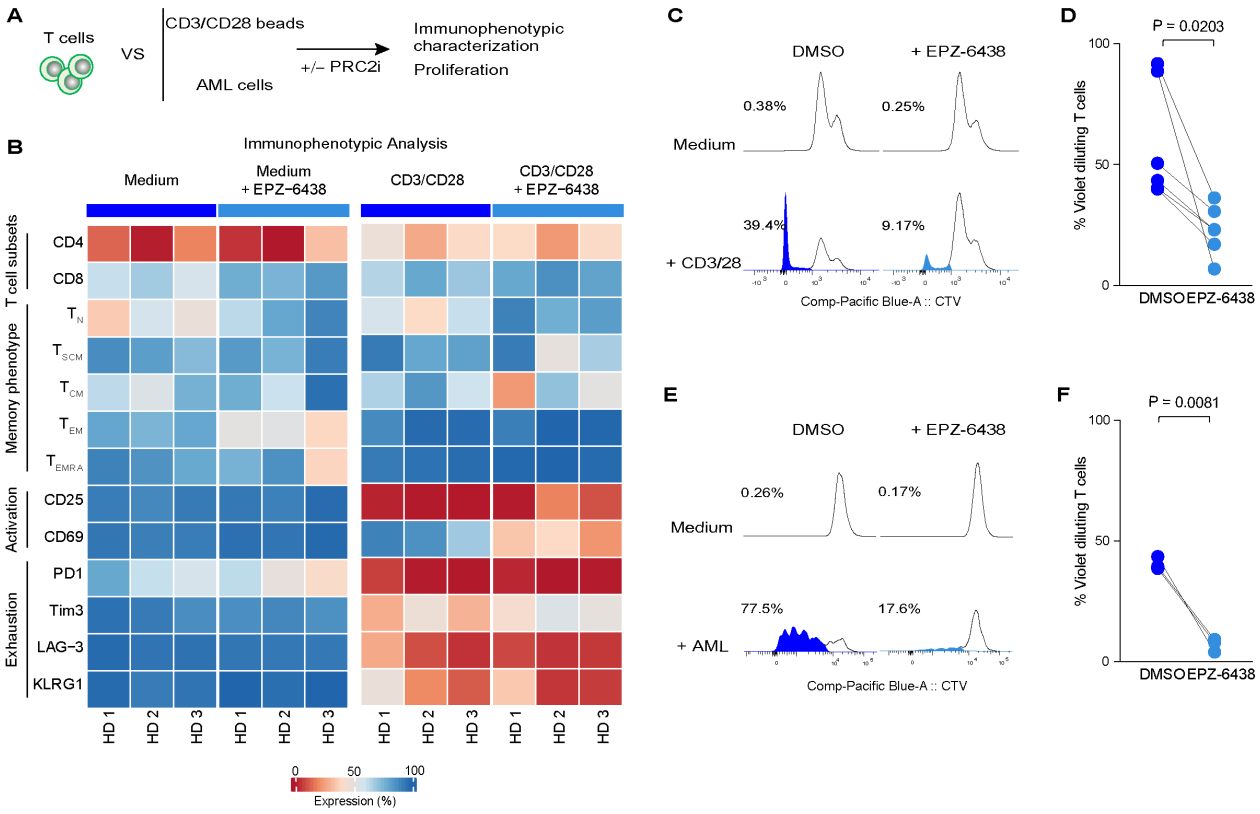

Supplementary Figure S9. Effects of EPZ-6438 on resting and activated human T cells. **A.** Outline of the experimental layout: T cells purified from healthy individuals were exposed or not to EPZ-6438 and either left resting, activated with CD3/CD28 beads or stimulated with allogeneic leukemia cells. After 7 days, T cell phenotype and proliferation were assessed. **B.** Heatmap summarizing the immunophenotypic characterization of T cells exposed or not to EPZ-6438 at 10 μM concentration, quantifying T cells subsets, memory phenotype (T_N: naïve, $CD45RA^+CD62L^+CD95^-$; T_{SCM}: stem cell memory, $CD45RA^+CD62L^+CD95^+$; T_{CM}: central memory, $CD45RA^-CD62L^+$; T_{EM}: effector memory, $CD45RA^-CD62L^-$; T_{EMRA}: effector memory re-expressing CD45RA, $CD45RA^+CD62L^-$), and expression of markers of activation (CD25 and CD69) and exhaustion (PD-1, Tim3, LAG-3, KLRG1). **C-D**. Representative plots (panel **C**) and summary graph (panel **D**) of proliferation assays performed stimulating T cells purified from healthy individuals with anti-CD/CD28 beads, and culturing them in presence or absence of EPZ-6438 at 10 μM concentration. Proliferation, measured by Cell Trace Violet (CTV) dilution, was determined at day 7 after stimulation. **E-F**. Representative plots (panel **E**) and summary graph (panel **F**) of proliferation assays performed stimulating T cells purified from healthy individuals with allogeneic AML blasts, and culturing them in presence or absence of EPZ-6438 at 10 μM concentration. Proliferation, measured by Cell Trace Violet (CTV) dilution, was determined at day 7 after stimulation.